Various rational solutions and rogue wave solutions of extended (2+1)-dimensional Calogero-Bogoyavlenskii-Schiff-like equation

Yueyang Feng, Sudao Bilige*

Department of Mathematics, Inner Mongolia University of Technology, Hohhot, 010051, PR China

Abstract In present paper, an original form of exact analytical solutions was introduced to solve nonlinear evolution equations by means of bilinear neural network method and symbolic computation. We gave high-order rational solutions including high-order lump-type solutions and higher-order rational solutions, periodic wave solutions, breather solutions and two kinds of rogue waves solutions of extended (2+1)-dimensional Calogero-Bogoyavlenskii-Schiff-like equation to exemplify the availability and advantage of the proposed approach which expand exact analytical solutions of nonlinear evolution equations. Meanwhile, physical properties and characters of the solutions were graphically shown through several groups of maps which are determined by special values.

Keywords: high-order rational solution, periodic wave solution, breather solution, rogue wave solution, bilinear neural network method

1 Introduction

Nonlinear evolution equations (NLEEs) is a generic term of nonlinear mathematical physical partial differential equation including variate t that can describe the evolution along with times in dynamics, physics, biology and other natural science. Recently, with the increasing development of technology and endeavor of numerous scholars, the study of solving NLEEs has aroused more and more attention, hence, there are various effective methods applied to solve NLEEs, such as homogeneous balance method [1], inverse scattering method [2], Bäcklund transformation [3], Darboux transformation [4], Hirota bilinear method [5] and simplest equation method [6]. In accordance with these methods, multiple rational solutions including lump solution [7, 8], lump-type solution [9], soliton solution [10], rogue wave solution [11], periodic solution [12, 13] and breather solution [14] are obtained.

Soliton is a stable solitary wave with constant speed, no deformation, no damage in interaction so that soliton theory has been widely studied in various domains while lump solution is a special type of rational function solutions which is localized in all directions of space compared with solitary wave solution. Ma [15, 16, 17, 18] proposed an approach to obtain lump solution directly by using symbolic computation has pushed lump solution to a new high. However, in the absence of external energy input, the wave train will evolve into a modulated wave train when the constituent waves of the wave train satisfied a certain relation, and with the appearance of self-focusing phenomenon, the maximum modulated amplitude may be far greater than the initial amplitude. Similarly, the occurrence of modulation instability is directly related to the characteristics of sea conditions. The steeper the wave is and the more concentrated the frequency distribution of the constituent wave is, the more likely the modulation instability

*Corresponding author. E-mail address: inmathematica@126.com(S.D. Bilige)

and rogue wave will be generated. Therefore, a increasing number of scholars have focused on the study of rogue waves and various rogue waves solutions have been obtain through symbolic computation [19, 20].

The study of neural networks have been around for a long time, Kohonen proposed that simple adaptive units make up the neural network which is a wide and interconnected network in 1988. The basic elements of the neural networks is neuron model, the neuron received input signal from other neuron, these input signal transmitted trough a weighted connection. This idea is similar to the method of solving NLEEs, thus, we introduced a method called bilinear neural network method based on neural network model and bilinear method to look for the solutions of NLEEs [21]. This method covers many methods of constructing a function after bilinearization to solve NLEEs that can be seen as models with only one hidden layer. For example, rogue wave solution, rational solution, lump solution, interaction solution, breather solution, periodic solitary wave solution [7]-[21], etc.

This article is divided into six parts. In section 2, bilinear neural network method and a new approach which solve NLEEs effectively will be introduced. In section 3, we will obtain the general bilinear form of extended (2+1)-dimensional Calogero-Bogoyavlenskii-Schiff equation by using general bilinear method and get extended (2+1)-dimensional Calogero-Bogoyavlenskii-Schiff-like (eCBSL) equation through transformation. Then, we obtain high-order lump-type solutions, higher-order rational solutions, periodic wave solutions, breather solutions of the equation through Maple. In section 4, by setting special values to coefficients of (2+1)-dimensional eCBSL equation, we will derive two kinds of rogue waves solutions of the equation. In section 5, several groups of maps including three-dimensional, contour and density plots will be provided to illustrate the dynamic properties and characters of these waves graphically. A few of conclusions and outlook will be given in the final section.

2 Bilinear neural network method

In this section, a l-hidden layer neural network model [see figure 1] which have a neurons of x_a, l-hidden layers of $G_{1,\rho}$, $G_{2,\gamma}, \ldots, G_{l,\mu}$, weight functions of w_{1c}, $w_{2d}, \ldots, w_{lp}$ and output layer of F_1, $F_2, \ldots, F_b$ will be plot, where a, b, c, d, l, p, ρ, γ and μ are natural numbers. As it shown, the l-hidden layer neural network has l hidden layer of G_l which are satisfied that the later hidden layer was obtained by the weighted sum of the previous hidden layer, through weighting sum the last hidden layer, the output layer of F_b will be derived.

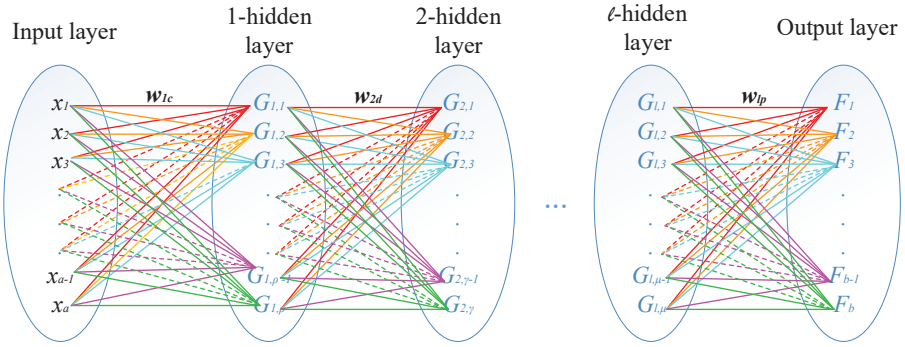

(a) 1

Figure 1: l-hidden layer neural network model

In order to obtain exact analytical solutions of NLEEs, we will construct a single-hidden layer neural network

model [see figure 2]. Taking the number of input neuron equal to L (L represents the dimension of space), thus, by taking the sum of x_L weighted by a_{ik}, the functions $G_N(\varphi_N)$ of hidden layer was obtained while taking the sum of x_L weighted by b_{jk} , the functions $g_M(\psi_M)$ of hidden layer was obtained, where $i = 1, 2, \ldots, N; j = 1, 2, \ldots, M$ and $k = 1, 2, \ldots, L$. At the same time, taking the number of functions in the output layer be one and through taking the sum of G_N and g_M weighted by 1 and m_j, the output function of f will be obtained.

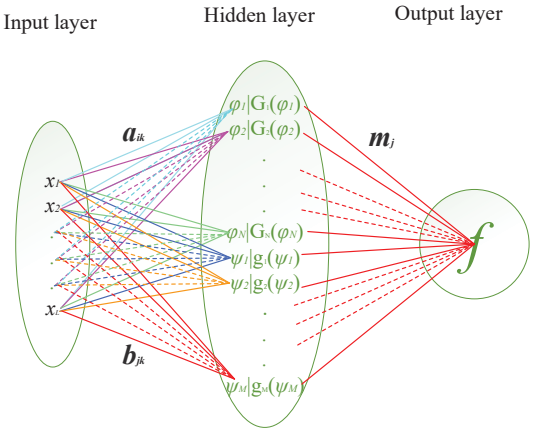

(a) 2

Figure 2: single-hidden layer neural network model

Step 1. According to the above model, we can construct the expression of f as follows [22],

$$f = a_0 + \sum_{i=1}^{N} \varphi_i^{2n_i} + \sum_{j=1}^{M} m_j g_j(\psi_j), \tag{1}$$

where

$$\varphi_i = a_{i0} + \sum_{k=1}^{L} a_{ik} x_k, \psi_j = b_{j0} + \sum_{k=1}^{L} b_{jk} x_k, \tag{2}$$

where $n_i \in \mathbb{N}$ and the weight coefficients of a_0, a_{ik}, b_{jk}, m_j $(i = 1, 2, \ldots, N; j = 1, 2, \ldots, M; k = 1, 2, \ldots, L)$ are real constants to be determined later. By choosing dependent variable transformation, we will obtain the general bilinear form of NLEEs.

Step 2. Substituting (1) and (2) into the general bilinear equation of NLEEs, we will obtain a polynomial about a_0, a_{ik}, b_{jk}, m_j and collect all wight coefficients of the terms with the same order. Then, taking the weight coefficients of different terms equal to zero, a group of nonlinear algebraic equations about a_0, a_{ik}, b_{jk}, m_j will be generated. We will solve the above nonlinear algebraic equations take the advantage of symbolic computation Maple.

Step 3. Substituting a_0, a_{ik}, b_{jk}, m_j into (1) and (2) and through variable transformation, we will obtain abundant solutions of NLEEs.

So as to obtaining high-order lump-type solutions, higher-order rational solutions, periodic wave solutions, breather solutions and rogue waves solutions to (2+1)-dimensional NLEEs, we hypothesize: $N = 3$, $M = 4$, $g_1(\psi_1) = e^{\psi_1}$, $g_2(\psi_2) = e^{-\psi_2}$ in (1) and $L = 3$, $x_1 = x, x_2 = y, x_3 = t$ in (2). The solution to general bilinear equation reads:

$$f = a_0 + \varphi_1^{2n_1} + \varphi_2^{2n_2} + \varphi_3^{2n_3} + m_1 e^{\psi_1} + m_2 e^{-\psi_2} + m_3 g_3(\psi_3) + m_4 g_4(\psi_4), \tag{3}$$

where $\varphi_i = a_{i0} + a_{i1}x + a_{i2}y + a_{i3}t$ $(i = 1, 2, 3)$, $\psi_i = b_{j0} + b_{j1}x + b_{j2}y + b_{j3}t$ $(j = 1, 2, 3, 4)$ satisfying $\prod_{i=1}^{3} a_{ik} \neq 0$ $(k = 1, 2, 3)$, $\prod_{k=1}^{3} a_{ik} \neq 0$ $(i = 1, 2, 3)$, $\prod_{j=1}^{3} b_{jk} \neq 0$ $(k = 1, 2, 3)$, $\prod_{k=1}^{3} b_{jk} \neq 0$ $(j = 1, 2, 3, 4)$.

Remark 2.1: If we choose $n_2 = n_1 = 1, a_{3k} = m_j = 0$ $(j = 1, 2, 3, 4; k = 0, 1, 2, 3)$, we will get lump solutions [23] of NLEEs. If we choose $n_2 = n_1 = m_1 = 1, a_{3k} = m_j = 0$, $(j = 2, 3, 4; k = 0, 1, 2, 3)$, we will get lump-kink solutions [24]. If we choose $n_2 = n_1 = 1, g_4(\psi_4) = \cosh\psi_4, a_{3k} = m_j = 0$ $(j = 1, 2, 3; k = 0, 1, 2, 3)$, we will get lump-hyperbolic cosine solutions [25]. If we choose $a_{ik} = m_j = 0$ $(j = 2, 3, 4; k = 0, 1, 2, 3)$, we will get 1-soliton solutions [26]. In a word, with the alter of the variate, we will obtain various kinds of solutions to NLEEs.

3 Various exact solutions to extended (2+1)-dimensional Calogero-Bogoyavlenskii-Schiff-like equation

We consider an extended (2+1)-dimensional Calogero-Bogoyavlenskii-Schiff (eCBS) equation:

$$u_{xt} + u_{xxxy} + 6u_{xx}u_y + 6u_x u_{xy} + \alpha u_{xy} + \beta u_{xx} + \delta u_{xxxx} + 12\delta u_x u_{xx} = 0, \tag{4}$$

where α, β, δ are arbitrary nonzero real parameters and $u = u(x, y, t)$.

Via dependent variable transformation

$$u = \ln f(x, y, t)_{xx}, \tag{5}$$

we can obtain the generalize bilinear form of equation (4) as follows:

$$\mathrm{GB}_{\mathrm{eCBS}} := (D_{p,x}D_{p,t} + D^3_{p,x}D_{p,y} + \alpha D_{p,x}D_{p,y} + \beta D^2_{p,x} + \delta D^4_{p,x})f \cdot f = 0, \tag{6}$$

where D is generalized bilinear differential operators [27] reads:

$$\begin{aligned} D^m_{p,x}D^n_{p,y}D^l_{p,t}f \cdot f &= (\partial_x + \chi_p\partial_{x'})^m(\partial_y + \chi_p\partial_{y'})^n(\partial_t + \chi_p\partial_{t'})^l f(x, y, t)f(x', y', t')\,|_{x=x',y=y',t=t'} \\ &= \sum_{i=0}^{m}\sum_{j=0}^{n}\sum_{k=0}^{l}\begin{pmatrix} m \\ i \end{pmatrix}\begin{pmatrix} n \\ j \end{pmatrix}\begin{pmatrix} l \\ k \end{pmatrix}\chi^i_p\chi^j_p\chi^k_p\frac{\partial^{m-i}}{\partial x^{m-i}}\frac{\partial^i}{\partial x'^i}\frac{\partial^{n-j}}{\partial y^{n-j}}\frac{\partial^j}{\partial y'^j}\frac{\partial^{l-k}}{\partial t^{l-k}}\frac{\partial^k}{\partial t'^k}\,|_{x=x',y=y',t=t'}\,, \end{aligned} \tag{7}$$

where $m, n, l \geq 0, \chi^s_p = (-1)^{r_p(s)}, s \equiv r_p(s) \bmod p$.

When taking $p = 3$, we can obtain the generalized bilinear eCBS equation:

$$\begin{aligned} \mathrm{GB}_{\mathrm{eCBS}} &:= (D_{3,x}D_{3,t} + D^3_{3,x}D_{3,y} + \alpha D_{3,x}D_{3,y} + \beta D^2_{3,x} + \delta D^4_{3,x})f \cdot f \\ &= 2ff_{xt} - 2f_t f_x + 6f_{xx}f_{xy} + 2\alpha(ff_{xy} - f_x f_y) + 2\beta(ff_{xx} - f^2_x) + 6\delta f^2_{xx} = 0. \end{aligned} \tag{8}$$

By applying transformation $u = \frac{f_x}{f}, v = \frac{f_y}{f}$, the generalized bilinear equation (8) is transformed into an extended (2+1)-dimensional Calogero-Bogoyavlenskii-Schiff-like (eCBSL) equation which has lump-soliton, lump-periodic, and lump-periodic-soliton solutions [28] as follows:

$$\mathrm{GP}_{\mathrm{eCBSL}} := u_t + 3u_x u_y + 3u^2 u_y + 3uu_x v + 3u^3 v + \alpha u_y + \beta u_x + 3\delta(u^2 + 2u_x)^2 = 0, \tag{9}$$

where $u_y = v_x$. Therefore, if f solves equation (8), $u(x, y, t) = \ln f(x, y, t)_{xx}$ will solve (2+1)-dimensional eCBSL equation (9). In this section, we will study diversely exact analytical solutions to equation (9).

3.1 High-order lump-type solutions

When $n_1 = 2, n_3 = n_2 = 1, m_j = 0$ $(j = 1, 2, 3, 4)$ in (3), (3) represents quartic function solutions of the generalized bilinear eCBS equation (8): $f = a_0 + \varphi_1^4 + \varphi_2^2 + \varphi_3^2$. According to Step 2 in the section 2, we get three classes of solutions.

$$\textbf{Case 1.1}: \beta = -\frac{\alpha a_{32} + a_{33}}{a_{31}}, \delta = -\frac{a_{32}}{a_{31}}, a_{11} = a_{10} = a_{21} = 0, a_{13} = -\alpha a_{12}, a_{22} = -\frac{a_{23}}{\alpha}, \alpha a_{31} \neq 0. \tag{10}$$

$$\textbf{Case 1.2}: a_{11} = a_{10} = 0, a_{13} = -\alpha a_{12}, a_{22} = -\frac{\alpha\delta a_{21}^2 + \alpha\delta a_{31}^2 - \beta a_{31}^2 - a_{33}a_{31}}{\alpha a_{21}},$$
$$a_{23} = \frac{(\alpha\delta - \beta)(a_{21}^2 + a_{31}^2) - a_{33}a_{31}}{a_{21}}, a_{32} = -\frac{\beta a_{31} + a_{33}}{\alpha}, a_{30} = \frac{a_{20}a_{31}}{a_{21}}, \alpha a_{21} \neq 0. \tag{11}$$

$$\textbf{Case 1.3}: a_{11} = a_{10} = 0, a_{13} = -\alpha a_{12}, a_{22} = -\frac{\delta a_{21}^2 + \delta a_{31}^2 + a_{32}a_{31}}{a_{21}}, a_{23} = \frac{\alpha\delta(a_{21}^2 + a_{31}^2) + \alpha a_{32}a_{31} - \beta a_{21}^2}{a_{21}},$$
$$a_{33} = -\alpha a_{32} - \beta a_{31}, a_{21} \neq 0, \tag{12}$$

where other parameters are arbitrary real constants. Through transformation (5), we obtain the high-order lump-type solutions of equation (9).

3.2 Higher-order rational solutions

I. When $n_1 = 4, n_2 = 2, n_3 = 1, m_j = 0$ $(j = 1, 2, 3, 4)$ in (3), (3) represents the solutions of the eighth function of equation (8): $f = a_0 + \varphi_1^8 + \varphi_2^4 + \varphi_3^2$. According to Step 2 in the section 2, we get five classes of solutions.

$$\textbf{Case 2.1}: a_{10} = a_{11} = a_{21}, \alpha = -\frac{a_{23}}{a_{22}}, \delta = -\frac{a_{22}(\beta a_{31} + a_{33})}{a_{23}a_{31}}, a_{13} = \frac{a_{23}a_{12}}{a_{22}}, a_{32} = \frac{a_{22}(\beta a_{31} + a_{33})}{a_{23}},$$
$$a_{12}a_{23}a_{31} \neq 0. \tag{13}$$

$$\textbf{Case 2.2}: a_{10} = a_{11} = a_{20} = a_{21}, \alpha = -\frac{a_{13}}{a_{12}}, \delta = -\frac{a_{12}(\beta a_{31} + a_{33})}{a_{13}a_{31}}, a_{23} = \frac{a_{13}a_{22}}{a_{12}}, a_{32} = \frac{a_{12}(\beta a_{31} + a_{33})}{a_{13}},$$
$$a_{12}a_{13}a_{31} \neq 0. \tag{14}$$

$$\textbf{Case 2.3}: a_{11} = a_{21} = 0, \beta = -\frac{\alpha a_{32} + a_{33}}{a_{31}}, \delta = -\frac{a_{32}}{a_{31}}, a_{13} = -\alpha a_{12}, a_{22} = -\frac{a_{23}}{\alpha}, \alpha a_{31} \neq 0. \tag{15}$$

$$\textbf{Case 2.4}: a_{11} = 0, \alpha = -\frac{a_{13}}{a_{12}}, \beta = -\frac{a_{12}a_{23}a_{31} - a_{13}a_{21}a_{32}}{a_{12}a_{21}a_{31}}, \delta = -\frac{a_{32}}{a_{31}}, a_{22} = \frac{a_{21}a_{32}}{a_{31}}, a_{33} = \frac{a_{23}a_{31}}{a_{21}},$$
$$a_{12}a_{21}a_{31} \neq 0. \tag{16}$$

$$\textbf{Case 2.5}: a_{11} = a_{31} = 0, \alpha = -\frac{a_{33}}{a_{32}}, \beta = \frac{a_{22}a_{33} - a_{23}a_{32}}{a_{32}a_{21}}, \delta = -\frac{a_{22}}{a_{21}}, a_{13} = \frac{a_{12}a_{33}}{a_{32}}, a_{32}a_{21} \neq 0, \tag{17}$$

where other parameters are arbitrary real constants. Through transformation (5), we obtain the higher-order rational solutions of equation (9).

Remark 3.2: We can get the same results as Case 2.1 - Case 2.5 when $(N = 3, n_1 = 3, n_2 = 2, n_1 = 1, m_j = 0)$, $(N = 3, n_1 = 5, n_2 = 2, n_1 = 1, m_j = 0)$, $(N = 3, n_1 = 6, n_2 = 2, n_1 = 1, m_j = 0)$ and $(N = 3, n_1 = 7, n_2 = 2, n_1 = 1, m_j = 0)$, we can get the same results as Case 2.2 - Case 2.5 when $(N = 3, n_1 = 5, n_2 = 3, n_1 = 1, m_j = 0)$, $(N = 3, n_1 = 6, n_2 = 3, n_1 = 1, m_j = 0)$, $(N = 3, n_1 = 5, n_2 = 4, n_1 = 1, m_j = 0)$ and $(N = 3, n_1 = 6, n_2 = 4, n_1 = 1, m_j = 0)$ other than the above.

II. When $n_1 = 5, n_2 = 3, n_3 = 1, m_j = 0$ $(j = 1, 2, 3, 4)$ in (3), (3) represents the solutions of the tenth function of equation (8): $f = a_0 + \varphi_1^{10} + \varphi_2^6 + \varphi_3^2$. According to Step 2 in the section 2, we get two classes of solutions.

$$\textbf{Case 2.6}: a_{11} = a_{21} = 0, \alpha = -\frac{a_{23}}{a_{22}}, \beta = -\frac{a_{22}a_{33} - a_{23}a_{32}}{a_{22}a_{31}}, \delta = -\frac{a_{32}}{a_{31}}, a_{13} = \frac{a_{23}a_{12}}{a_{22}}, a_{22}a_{31} \neq 0. \tag{18}$$

$$\textbf{Case 2.7}: a_{11}=a_{20}=0, \alpha=-\frac{a_{13}}{a_{12}}, \beta=-\frac{a_{12}a_{33}-a_{13}a_{32}}{a_{12}a_{31}}, \delta=-\frac{a_{32}}{a_{31}}, a_{22}=\frac{a_{21}a_{32}}{a_{31}}, a_{23}=\frac{a_{21}a_{33}}{a_{31}},$$
$$a_{12}a_{31}\neq 0, \tag{19}$$

where other parameters are arbitrary real constants. Through transformation (5), we obtain the higher-order rational solutions of equation (9).

Remark 3.3: We can get the same results as Case 2.6 and Case 2.7 when $(N=3, n_1=6, n_2=3, n_1=1, m_j=0)$, $(N=3, n_1=5, n_2=4, n_1=1, m_j=0)$ and $(N=3, n_1=6, n_2=4, n_1=1, m_j=0)$ other than the above.

3.3 Periodic wave solutions

I. When $a_{ik}=0$, $m_4=m_3=m_2=m_1$, $\psi_2=\psi_1$, $g_3(\psi_3)=\tan\psi_3, g_4(\psi_4)=\tanh\psi_4$ in (3), (3) represents the solutions of equation (8): $f=a_0+m_1e^{\psi_1}+m_1e^{-\psi_1}+m_1\tan\psi_3+m_1\tanh\psi_4$. According to Step 2 in the section 2, we get ten classes of solutions.

$$\textbf{Case 3.1}: b_{11}=b_{31}=0, \delta=-\frac{b_{42}}{b_{41}}, b_{13}=-\alpha b_{12}, b_{33}=-\alpha b_{32}, b_{43}=-\alpha b_{42}-\beta b_{41}, b_{41}\neq 0. \tag{20}$$

$$\textbf{Case 3.2}: b_{11}=b_{41}=0, \delta=-\frac{b_{32}}{b_{31}}, b_{13}=-\alpha b_{12}, b_{33}=-\alpha b_{32}-\beta b_{31}, b_{43}=-\alpha b_{42}, b_{31}\neq 0. \tag{21}$$

$$\textbf{Case 3.3}: b_{31}=b_{41}=0, \delta=-\frac{b_{12}}{b_{11}}, b_{13}=-\alpha b_{12}-\beta b_{11}, b_{33}=-\alpha b_{32}, b_{43}=-\alpha b_{42}, b_{11}\neq 0. \tag{22}$$

$$\textbf{Case 3.4}: b_{41}=0, \delta=-\frac{b_{32}}{b_{31}}, b_{12}=\frac{b_{32}b_{11}}{b_{31}}, b_{13}=-\frac{b_{11}(\alpha b_{32}+\beta b_{31})}{b_{31}}, b_{33}=-\alpha b_{32}-\beta b_{31}, b_{43}=-\alpha b_{42},$$
$$b_{31}\neq 0. \tag{23}$$

$$\textbf{Case 3.5}: b_{31}=0, \delta=-\frac{b_{42}}{b_{41}}, b_{12}=\frac{b_{42}b_{11}}{b_{41}}, b_{13}=-\frac{b_{11}(\alpha b_{42}+\beta b_{41})}{b_{41}}, b_{33}=-\alpha b_{32}, b_{43}=-\alpha b_{42}-\beta b_{41},$$
$$b_{41}\neq 0. \tag{24}$$

$$\textbf{Case 3.6}: b_{31}=0, \delta=-\frac{b_{12}}{b_{11}}, b_{13}=-\alpha b_{12}-\beta b_{11}, b_{33}=-\alpha b_{32}, b_{42}=\frac{b_{12}b_{41}}{b_{11}}, b_{43}=-\frac{b_{41}(\alpha b_{12}+\beta b_{11})}{b_{11}},$$
$$b_{11}\neq 0. \tag{25}$$

$$\textbf{Case 3.7}: b_{41}=0, \delta=-\frac{b_{12}}{b_{11}}, b_{13}=-\alpha b_{12}-\beta b_{11}, b_{32}=\frac{b_{12}b_{31}}{b_{11}}, b_{33}=-\frac{b_{31}(\alpha b_{12}+\beta b_{11})}{b_{11}}, b_{43}=-\alpha b_{42},$$
$$b_{11}\neq 0. \tag{26}$$

$$\textbf{Case 3.8}: b_{11}=0, \delta=-\frac{b_{32}}{b_{31}}, b_{13}=-\alpha b_{12}, b_{33}=-\alpha b_{32}-\beta b_{31}, b_{42}=\frac{b_{32}b_{41}}{b_{31}}, b_{43}=-\frac{b_{41}(\alpha b_{32}+\beta b_{31})}{b_{31}},$$
$$b_{31}\neq 0. \tag{27}$$

$$\textbf{Case 3.9}: a_0=0, \delta=-\frac{b_{32}}{b_{31}}, b_{12}=\frac{b_{32}b_{11}}{b_{31}}, b_{13}=-\frac{b_{11}(\alpha b_{32}+\beta b_{31})}{b_{31}}, b_{33}=-\alpha b_{32}-\beta b_{31}, b_{42}=\frac{b_{32}b_{41}}{b_{31}},$$
$$b_{43}=-\frac{b_{41}(\alpha b_{32}+\beta b_{31})}{b_{31}}, b_{31}\neq 0. \tag{28}$$

$$\textbf{Case 3.10}: \delta=-\frac{b_{12}}{b_{11}}, b_{13}=-\alpha b_{12}-\beta b_{11}, b_{32}=\frac{b_{12}b_{31}}{b_{11}}, b_{33}=-\frac{b_{31}(\alpha b_{12}+\beta b_{11})}{b_{11}}, b_{42}=\frac{b_{12}b_{41}}{b_{11}},$$
$$b_{43}=-\frac{b_{41}(\alpha b_{12}+\beta b_{11})}{b_{11}}, b_{11}\neq 0, \tag{29}$$

where other parameters are arbitrary real constants. Through transformation (5), we obtain the periodic wave solutions of equation (9).

Remark 3.4: In addition, we can get the same results other than the above as follows:

When $m_4\neq m_3\neq m_2\neq m_1$ $(f=a_0+m_1e^{\psi_1}+m_2e^{-\psi_1}+m_3\tan\psi_3+m_4\tanh\psi_4)$, we get the same results as Case 3.1 - Case 3.5.

When $m_4 \neq m_3 \neq m_2 \neq m_1$, $\psi_3 = \psi_2 = \psi_1$ ($f = a_0 + m_1 e^{\psi_1} + m_2 e^{-\psi_1} + m_3 \tan\psi_1 + m_4 \tanh\psi_4$), we get the same results as Case 3.2 - Case 3.4.

When $m_4 \neq m_3 \neq m_2 \neq m_1$, $\psi_4 = \psi_3 = \psi_2 = \psi_1$ ($f = a_0 + m_1 e^{\psi_1} + m_2 e^{-\psi_1} + m_3 \tan\psi_1 + m_4 \tanh\psi_1$), we get the same result as Case 3.3.

When $g_3(\psi_3) = \cos\psi_3, g_4(\psi_4) = \cosh\psi_4$ ($f = a_0 + m_1 e^{\psi_1} + m_1 e^{-\psi_1} + m_1 \cos\psi_3 + m_1 \cosh\psi_4$) and $g_3(\psi_3) = \cos\psi_3, g_4(\psi_4) = \sin\psi_4$ ($f = a_0 + m_1 e^{\psi_1} + m_1 e^{-\psi_1} + m_1 \cos\psi_3 + m_1 \sin\psi_4$), we get the same results as Case 3.3 - Case 3.5.

When $m_4 = 0$, $m_3 \neq m_2 \neq m_1$, $\psi_2 \neq \psi_1$, $g_3(\psi_3) = \cos\psi_3$ ($f = a_0 + m_1 e^{\psi_1} + m_2 e^{-\psi_2} + m_3 \cos\psi_3$), we get the same results as Case 3.1, Case 3.3, Case 3.4, Case 3.6, Case 3.10.

II. When $a_{ik} = 0$, $m_2 = m_1$, $\psi_2 = \psi_1$, $g_3(\psi_3) = \cos\psi_3$, $g_4(\psi_4) = \sin\psi_4$ in (3), (3) represents the solutions of equation (8): $f = a_0 + m_1 e^{\psi_1} + m_1 e^{-\psi_1} + m_3 \cos\psi_3 + m_4 \sin\psi_4$. According to Step 2 in the section 2, we get seven classes of solutions.

$$\textbf{Case 3.11}: \delta = -\frac{b_{12}}{b_{11}}, b_{13} = \frac{3b_{12}b_{11}^2}{2} - \frac{(3b_{11}^2 + 2\alpha)b_{12}}{2} - \beta b_{11}, b_{32} = \frac{b_{12}b_{31}}{b_{11}}, b_{33} = -\frac{\alpha b_{12}b_{31}}{b_{11}} - \beta b_{31},$$
$$b_{42} = \frac{b_{12}b_{41}}{b_{11}}, b_{43} = -\frac{\alpha b_{12}b_{41}}{b_{11}} - \beta b_{41}, b_{11} \neq 0. \tag{30}$$

$$\textbf{Case 3.12}: b_{41} = 0, b_{11} = \frac{b_{13}}{\alpha\delta - \beta}, b_{12} = \frac{\delta b_{13}}{\alpha\delta - \beta}, b_{31} = \frac{b_{33}}{\alpha\delta - \beta}, b_{32} = -\frac{\delta b_{13}}{\alpha\delta - \beta}, b_{42} = -\frac{b_{43}}{\alpha},$$
$$\alpha(\alpha\delta - \beta) \neq 0. \tag{31}$$

$$\textbf{Case 3.13}: b_{31} = 0, b_{11} = \frac{b_{13}}{\alpha\delta - \beta}, b_{12} = \frac{\delta b_{13}}{\alpha\delta - \beta}, b_{32} = -\frac{b_{33}}{\alpha}, b_{41} = \frac{b_{43}}{\alpha\delta - \beta}, b_{42} = -\frac{\delta b_{43}}{\alpha\delta - \beta},$$
$$\alpha(\alpha\delta - \beta) \neq 0. \tag{32}$$

$$\textbf{Case 3.14}: b_{31} = b_{41} = 0, b_{11} = \frac{b_{13}}{\alpha\delta - \beta}, b_{12} = \frac{\delta b_{13}}{\alpha\delta - \beta}, b_{32} = -\frac{b_{33}}{\alpha}, b_{42} = -\frac{b_{43}}{\alpha}, \alpha(\alpha\delta - \beta) \neq 0. \tag{33}$$

$$\textbf{Case 3.15}: b_{11} = 0, b_{12} = -\frac{b_{13}}{\alpha}, b_{31} = \frac{b_{33}}{\alpha\delta - \beta}, b_{32} = -\frac{\delta b_{33}}{\alpha\delta - \beta}, b_{41} = \frac{b_{43}}{\alpha\delta - \beta}, b_{42} = -\frac{\delta b_{43}}{\alpha\delta - \beta},$$
$$\alpha(\alpha\delta - \beta) \neq 0. \tag{34}$$

$$\textbf{Case 3.16}: b_{11} = b_{41} = 0, b_{12} = -\frac{b_{13}}{\alpha}, b_{31} = \frac{b_{33}}{\alpha\delta - \beta}, b_{32} = -\frac{\delta b_{33}}{\alpha\delta - \beta}, b_{42} = -\frac{b_{43}}{\alpha}, \alpha(\alpha\delta - \beta) \neq 0. \tag{35}$$

$$\textbf{Case 3.17}: b_{11} = b_{31} = 0, b_{12} = -\frac{b_{13}}{\alpha}, b_{32} = -\frac{b_{33}}{\alpha}, b_{41} = \frac{b_{43}}{\alpha\delta - \beta}, b_{42} = -\frac{\delta b_{43}}{\alpha\delta - \beta}, \alpha(\alpha\delta - \beta) \neq 0, \tag{36}$$

where other parameters are arbitrary real constants. Through transformation (5), we obtain the periodic wave solutions of equation (9).

Remark 3.5: We can get the same results as Case 3.15 - Case 3.17 when $m_4 = m_3 = m_2 = m_1$ ($f = a_0 + m_1 e^{\psi_1} + m_1 e^{-\psi_1} + m_1 \cos\psi_3 + m_1 \sin\psi_4$) and when $m_4 = m_3 = m_2 = m_1$, $g_4(\psi_4) = \cosh\psi_4$ ($f = a_0 + m_1 e^{\psi_1} + m_1 e^{-\psi_1} + m_1 \cos\psi_3 + m_1 \cosh\psi_4$), we can get the same result as Case 3.11 when $m_4 = m_3 = m_2 = m_1$, $\psi_4 = \psi_3$ ($f = a_0 + m_1 e^{\psi_1} + m_1 e^{-\psi_1} + m_1 \cos\psi_3 + m_1 \sin\psi_3$) other than the above.

3.4 Breather solutions

When $a_{ik} = 0$, $m_4 = 0$, $g_3(\psi_3) = \cos\psi_3$ in (3), (3) represents solutions of equation (8): $f = a_0 + m_1 e^{\psi_1} + m_2 e^{-\psi_2} + m_3 \cos\psi_3$. According to Step 2 in the section 2, we get two classes of solutions.

$$\textbf{Case 4.1}: b_{11} = 0, \delta = -\frac{b_{32}}{b_{31}}, b_{13} = -\alpha b_{12}, b_{22} = \frac{b_{21}b_{32}}{b_{31}}, b_{23} = -\frac{b_{21}(\alpha b_{32} + \beta b_{31})}{b_{31}}, b_{33} = -\alpha b_{32} - \beta b_{31},$$
$$b_{31} \neq 0. \tag{37}$$

$$\textbf{Case 4.2}: \delta = -\frac{b_{32}}{b_{31}}, b_{12} = \frac{b_{11}b_{32}}{b_{31}}, b_{13} = -\frac{b_{11}(\alpha b_{32}+\beta b_{31})}{b_{31}}, b_{22} = \frac{b_{21}b_{32}}{b_{31}}, b_{23} = -\frac{b_{21}(\alpha b_{32}+\beta b_{31})}{b_{31}},$$
$$b_{33} = -\alpha b_{32} - \beta b_{31}, b_{31} \neq 0, \tag{38}$$

where other parameters are arbitrary real constants. Through transformation (5), we obtain the breather solutions of equation (9).

4 Rogue waves solutions

In order to derive rogue waves solutions to (2+1)-dimensional eCBSL equation, we can set special values for α, β, δ, for instance, if set $\alpha = 1$ in equation (9), we will obtain:

$$\mathrm{GP}_{\mathrm{eCBSL}} := u_t + 3u_x u_y + 3u^2 u_y + 3uu_x v + 3u^3 v + u_y + \beta u_x + 3\delta(u^2 + 2u_x)^2 = 0. \tag{39}$$

The corresponding generalize bilinear equation reads:

$$\begin{aligned}\mathrm{GB}_{\mathrm{eCBS}} &:= (D_{3,x}D_{3,t} + D_{3,x}^3 D_{3,y} + \alpha D_{3,x}D_{3,y} + \beta D_{3,x}^2 + \delta D_{3,x}^4) f \cdot f \\ &= 2ff_{xt} - 2f_t f_x + 6f_{xx}f_{xy} + 2(ff_{xy} - f_x f_y) + 2\beta(ff_{xx} - f_x^2) + 6\delta f_{xx}^2 = 0.\end{aligned} \tag{40}$$

I. When $n_1 = 4, n_2 = 2, n_3 = 1$, $m_4 = m_3 = m_2 = m_1$, $\psi_4 = \psi_3 = \psi_2 = \psi_1$, $g_3(\psi_1) = \cos\psi_1, g_4(\psi_1) = \sin\psi_1$ in (3), (3) represents rogue waves solutions of equation (40): $f = a_0 + \varphi_1^8 + \varphi_2^4 + \varphi_3^2 + m_1 e^{\psi_1} + m_1 e^{-\psi_1} + m_1\cos\psi_1 + m_1\sin\psi_1$. According to Step 2 in the section 2, we get five classes of solutions.

$$\textbf{Case 5.1}: a_{11} = a_{10} = a_{21} = b_{11} = 0, \beta = -\frac{a_{32}+a_{33}}{a_{31}}, \delta = -\frac{a_{32}}{a_{31}}, a_{12} = -a_{13}, a_{22} = -a_{23}, b_{12} = -b_{13},$$
$$a_{31} \neq 0. \tag{41}$$

$$\textbf{Case 5.2}: a_{11} = a_{10} = a_{21} = 0, \beta = -\frac{a_{31}b_{12} + a_{33}b_{11}}{a_{31}b_{11}}, \delta = -\frac{b_{42}}{b_{11}}, a_{12} = -a_{13}, a_{22} = -a_{23}, a_{32} = \frac{a_{31}b_{12}}{b_{11}},$$
$$b_{11} \neq 0. \tag{42}$$

$$\textbf{Case 5.3}: a_{11} = a_{10} = a_{21} = 0, \beta = -\frac{a_{31}b_{13} + a_{32}b_{11}}{a_{31}b_{11}}, \delta = -\frac{a_{32}}{a_{31}}, a_{22} = -a_{23}, a_{33} = \frac{a_{31}b_{13}}{b_{11}}, b_{12} = \frac{a_{32}b_{11}}{a_{31}},$$
$$b_{11}a_{31} \neq 0. \tag{43}$$

$$\textbf{Case 5.4}: a_{11} = a_{10} = a_{21} = b_{11} = 0, \delta = -\frac{a_{32}}{a_{31}}, a_{12} = -a_{13}, a_{22} = -a_{23}, a_{33} = -a_{31}\beta - a_{32}, b_{12} = -b_{13},$$
$$a_{31} \neq 0. \tag{44}$$

$$\textbf{Case 5.5}: a_{11} = a_{10} = a_{21} = 0, \delta = -\frac{b_{12}}{b_{11}}, a_{22} = -a_{23}, a_{32} = \frac{a_{31}b_{12}}{b_{11}}, a_{33} = -\frac{a_{31}(\beta b_{11} + b_{12})}{b_{11}}, b_{13} = -\beta b_{11} - b_{12},$$
$$b_{11} \neq 0, \tag{45}$$

where other parameters are arbitrary real constants. Through transformation (5), we obtain one class rogue waves solutions of equation (39).

Remark 4.1: We can get the same results as Case 5.4 and Case 5.5 when $g_4(\psi_1) = \sinh\psi_1$ ($f = a_0 + \varphi_1^8 + \varphi_2^4 + \varphi_3^2 + m_1 e^{\psi_1} + m_1 e^{-\psi_1} + m_1\cos\psi_1 + m_1\sinh\psi_1$), when $g_4(\psi_1) = \cosh\psi_1$ ($f = a_0 + \varphi_1^8 + \varphi_2^4 + \varphi_3^2 + m_1 e^{\psi_1} + m_1 e^{-\psi_1} + m_1\cos\psi_1 + m_1\cosh\psi_1$), when $m_4 = 0$ ($f = a_0 + \varphi_1^8 + \varphi_2^4 + \varphi_3^2 + m_1 e^{\psi_1} + m_1 e^{-\psi_1} + m_1\cos\psi_1$) and when $m_4 = m_3 = 0$ ($f = a_0 + \varphi_1^8 + \varphi_2^4 + \varphi_3^2 + m_1 e^{\psi_1} + m_1 e^{-\psi_1}$) other than the above. In addition, we can get the same results as Case 5.1 and Case 5.2 when $g_3(\psi_3) = \cos\psi_3, g_4(\psi_4) = \sin\psi_4$ ($f = a_0 + \varphi_1^8 + \varphi_2^4 + \varphi_3^2 + m_1 e^{\psi_1} + m_1 e^{-\psi_1} + m_1\cos\psi_3 + m_1\sin\psi_4$).

II. When $n_1 = 2, n_3 = n_2 = 1$, $m_4 = m_3 = m_2 = 1$, $\psi_4 = \psi_3 = \psi_2 = \psi_1$, $g_3(\psi_1) = \tan\psi_1, g_4(\psi_1) = \tanh\psi_1$ in (3), (3) represents rogue waves solutions of equation (40): $f = a_0 + \varphi_1^4 + \varphi_2^2 + \varphi_3^2 + m_1 e^{\psi_1} + e^{-\psi_1} + \tan\psi_1 + \tanh\psi_1$. According to Step 2 in the section 2, we get three classes of solutions.

$$\textbf{Case 6.1}: a_{11} = a_{10} = a_{21} = b_{11} = 0, \beta = -\frac{a_{32} + a_{33}}{a_{31}}, \delta = -\frac{a_{32}}{a_{31}}, a_{12} = -a_{13}, a_{22} = -a_{23}, a_{31} \neq 0. \tag{46}$$

$$\textbf{Case 6.2}: a_{11} = a_{10} = b_{11} = 0, a_{12} = -a_{13}, a_{22} = \frac{(\beta-\delta)a_{31}^2 - \delta a_{21}^2 + a_{33}a_{31}}{a_{21}},$$
$$a_{23} = -\frac{(\beta-\delta)(a_{21}^2 + a_{31}^2) + a_{33}a_{31}}{a_{21}}, a_{32} = -\beta a_{31} - a_{33}, a_{30} = \frac{a_{20}a_{31}}{a_{21}}, b_{12} = -b_{13}, a_{21} \neq 0.$$

$$\textbf{Case 6.3}: a_{11} = a_{10} = b_{11} = 0, a_{12} = -a_{13}, a_{22} = -\frac{\delta(a_{31}^2 + a_{21}^2) + a_{32}a_{31}}{a_{21}}, a_{23} = -\frac{(\beta-\delta)a_{21}^2 - \delta a_{31}^2 + a_{32}a_{31}}{a_{21}},$$
$$a_{33} = -\beta a_{31} - a_{32}, b_{12} = -b_{13}, a_{21} \neq 0, \tag{47}$$

where other parameters are arbitrary real constants. Through transformation (5), we obtain the rogue waves solutions of equation (39).

Remark 4.2: We can get the same results as Case 6.1 - Case 6.3 when $g_3(\psi_1) = \cos\psi_1, g_4(\psi_1) = \cosh\psi_1$ ($f = a_0 + \varphi_1^4 + \varphi_2^2 + \varphi_3^2 + m_1 e^{\psi_1} + e^{-\psi_1} + \cos\psi_1 + \cosh\psi_1$) and $g_3(\psi_1) = \sin\psi_1, g_4(\psi_1) = \sinh\psi_1$ ($f = a_0 + \varphi_1^4 + \varphi_2^2 + \varphi_3^2 + m_1 e^{\psi_1} + e^{-\psi_1} + \sin\psi_1 + \sinh\psi_1$).

5 Dynamic properties

In this section, we will study the dynamic properties of the above solutions, multifarious three-dimensional plots, contour and density maps for (2+1)-dimensional eCBSL equation are depicted.

5.1 Three-dimensional, contour and density plots of the solution to Case 1.1

If we substitute Case 1.1 into equation (3), the solution f_1 to (2+1)-dimensional eCBSL equation as follows:

$$f_1 = a_0 + (-\alpha a_{12} t + a_{12} y)^4 + (a_{23} t - \frac{a_{23} y}{\alpha} + a_{20})^2 + (a_{31} x + a_{32} y + a_{33} t + a_{30})^2.$$

Through transformation (5), we can derive high-order lump-type solution of equation (9) as follows:

$$u_1 = \frac{2a_{31}^2}{f_1} - \frac{4a_{31}^2 \psi_3^2}{f_1^2},$$

where $\psi_3 = a_{31} x + a_{32} y + a_{33} t + a_{30}$ and $a_0, a_{12}, a_{23}, a_{20}, a_{31}, a_{32}, a_{33}, a_{30}$ are arbitrary real numbers.

We choose particular values to illustrate the high-order lump-type solution to (2+1)-dimensional eCBSL equation:

$$\alpha = 1, a_0 = 4, a_{12} = 2, a_{23} = 1, a_{20} = 4, a_{31} = 5, a_{32} = 3, a_{33} = 2, a_{30} = 5. \tag{48}$$

Through selecting appropriate values for the parameters, the dynamic characters and structures of the high-order lump-type solution are vividly shown in figure 3 which contained the three-dimensional plots [see figure 3(a,b,c)] that exhibit the localized structures and we adopt the same color for the points that $x + y$ are identical and and density maps [see figure 3(d,e,f)] in the (x, y)-plane that reflect the energy distribution when t = -10, 0, 10. It is clear that the wave is keep moving with the shape unchanged.

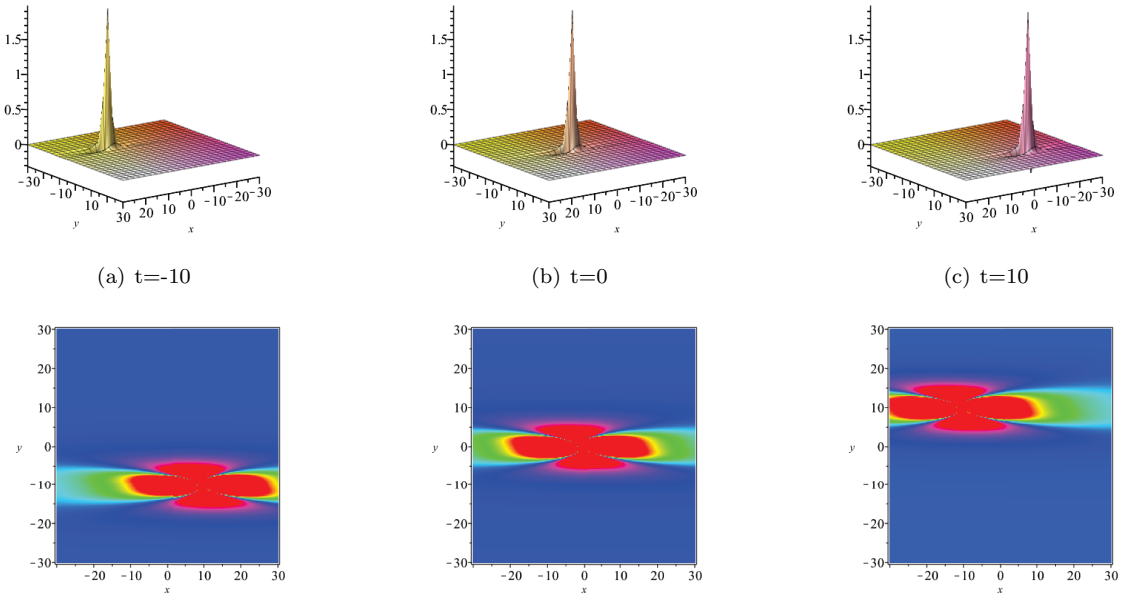

(a) t=-10 (b) t=0 (c) t=10

(d) t=-10 (e) t=0 (f) t=10

Figure 3: Three-dimensional plots, contour and density plots of the wave with the parameters (48) at times t = -10, 0, 10.

5.2 Three-dimensional and contour plots of the solution to Case 4.2

If we substitute Case 4.2 into equation (3), the solution f_2 to (2+1)-dimensional eCBSL equation as follows:

$$f_2 = a_0 + m_1 e^{-\frac{b_{11}(\alpha b_{32}+\beta b_{31})}{b_{31}}+b_{11}x+\frac{b_{11}b_{32}y}{b_{31}}+b_{10}} + m_2 e^{\frac{b_{21}(\alpha b_{32}+\beta b_{31})}{b_{31}}-b_{21}x-\frac{b_{21}b_{32}y}{b_{31}}-b_{20}}$$
$$+ m_3\cos((\alpha b_{32}+\beta b_{31})t - b_{31}x - b_{32}y - b_{30}).$$

Through transformation (5), we can derive breather solution of equation (9) as follows:

$$u_2 = \frac{1}{f_2^2}(-m_1^2 b_{21}^2 e^{-2\psi_2} + 2m_1 m_2 b_{11} b_{21} e^{\psi_1-\psi_2} + (2m_2 m_3 b_{21} b_{31}\sin\psi_3 + b_{21} f_2)e^{-\psi_2} + m_3^2 b_{31}^2\cos\psi_3^2$$
$$- 2m_1 m_2 b_{11} b_{31} e^{\psi_1}\sin\psi_3 - m_3 b_{31}^2 f_2\cos\psi_3 + m_1 b_{11}^2 f_2 e^{\psi_1} - m_1^2 b_{11}^2 e^{2\psi_1} - m_3^2 b_{31}^2),$$

where $\psi_1 = -\frac{b_{11}(\alpha b_{32}+\beta b_{31})}{b_{31}} + b_{11}x + \frac{b_{11}b_{32}y}{b_{31}} + b_{10}$, $\psi_2 = -\frac{b_{21}(\alpha b_{32}+\beta b_{31})}{b_{31}} + b_{21}x + \frac{b_{21}b_{32}y}{b_{31}} + b_{20}$, $\psi_3 = (\alpha b_{32}+\beta b_{31})t - b_{31}x - b_{32}y - b_{30}$ and $a_0, b_{10}, b_{11}, b_{20}, b_{21}, b_{30}, b_{31}, b_{32}$ are arbitrary real numbers.

We choose particular values to illustrate breather solution to (2+1)-dimensional eCBSL equation:

$$\alpha = 1, \beta = 1, m_1 = 2, m_2 = 3, m_3 = 2, a_0 = 1, b_{10} = 6, b_{11} = 2, b_{20} = 6, b_{21} = 3, b_{30} = 2, b_{31} = 10, b_{32} = 2. \quad (49)$$

Dynamical behaviors of breather solution along with the time evolution is depicted in figure 4 including three-dimensional plots [see figure 4(a, b, c)] and contour maps [see figure 4(d, e, f)]. These waves are mutual independence and remain parallel at times t = -10, 0, 10. If setting the different values in f_2, we will obtain different shape of waves, at the same time, we can choose t freely to illustrate the dynamic characters of the solutions clearly with the aid of Maple. It is obvious that the waves are keep moving finely.

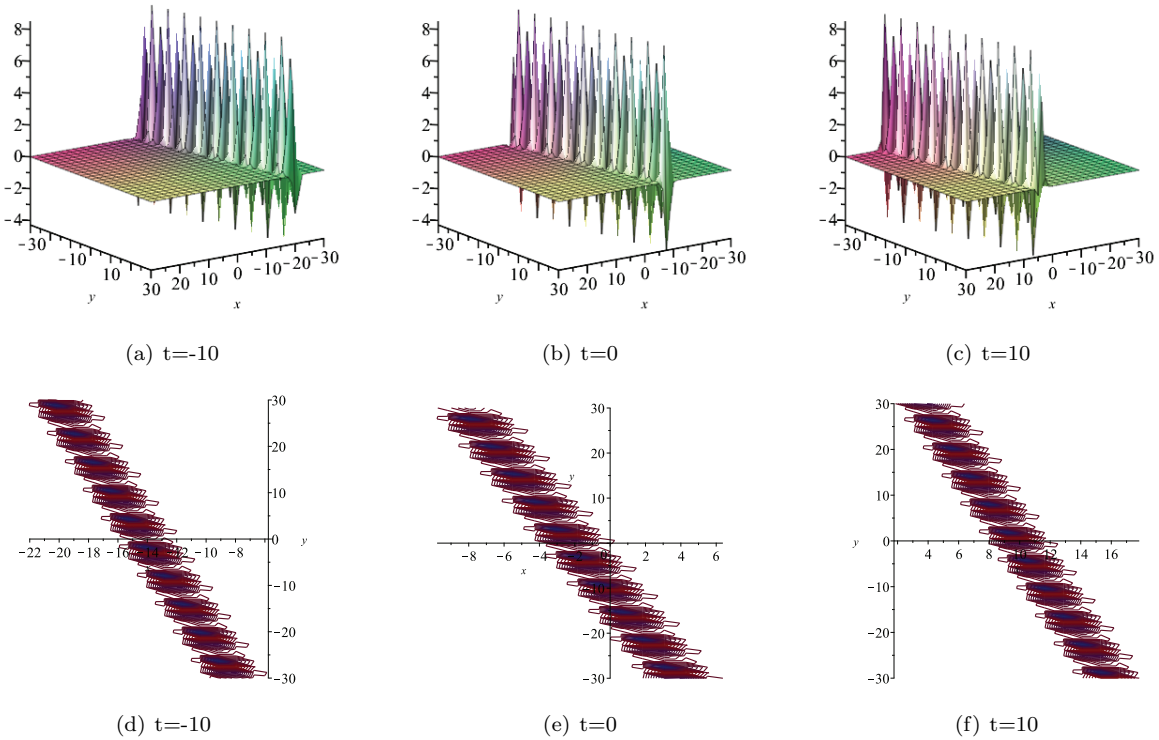

(a) t=-10 (b) t=0 (c) t=10

(d) t=-10 (e) t=0 (f) t=10

Figure 4: Three-dimensional plots and contour maps of the wave with the parameters (49) at times t = -10, 0, 10.

5.3 Three-dimensional and contour plots of the solution to Case 5.5

If we substitute Case 5.5 into equation (3), the solution f_3 to (2+1)-dimensional eCBSL equation as follows:

$$\begin{aligned} f_3 = {} & a_0 + (a_{13}t - a_{13}y)^8 + (a_{23}t - a_{23}y + a_{20})^4 + (a_{31}x + \frac{a_{31}b_{12}}{b_{11}}y - \frac{a_{31}(b_{11}\beta + b_{12})}{b_{11}}t + a_{30})^2 \\ & + m_1 e^{b_{11}x + b_{12}y - (\beta b_{11} + b_{12})t + b_{10}} + m_1 e^{-b_{11}x - b_{12}y + (\beta b_{11} + b_{12})t - b_{10}} \\ & + m_1 \cos(b_{11}x + b_{12}y - (\beta b_{11} + b_{12})t + b_{10}) + m_1 \sin(b_{11}x + b_{12}y - (\beta b_{11} + b_{12})t + b_{10}). \end{aligned}$$

Through transformation (5), we can derive rogue waves solutions of equation (39) as follows:

$$\begin{aligned} u_3 = \frac{1}{f_3^2}[& m_1^2 b_{11}^2((\cos(-\psi_1) + 2\sin(-\psi_1))e^{-\psi_1} - 2e^{-2\psi_1} - 2e^{\psi_1}(\cos(-\psi_1) - 1) - \sin(-2\psi_1) - 1) \\ & + m_1 a_{31} b_{11}(4\varphi_3 e^{-\psi_1} - 4e^{\psi_1} - 2\varphi_3\cos(-\psi_1) - 4\varphi_3\sin(-\psi_1)) - 4a_{31}^2\varphi_3^2 + 2a_{31}^2 f_3 \\ & + m_1 b_{11}^2 f_3(e^{\psi_1} + e^{-\psi_1} + \sin(-\psi_1) - \cos(-\psi_1))], \end{aligned}$$

where $\varphi_3 = a_{31}x + \frac{a_{31}b_{12}}{b_{11}}y - \frac{a_{31}(b_{11}\beta + b_{12})}{b_{11}}t + a_{30}$, $\psi_1 = b_{11}x + b_{12}y - (\beta b_{11} + b_{12})t + b_{10}$ and $a_0, a_{13}, a_{23}, a_{20}, a_{31}, a_{30}$, b_{11}, b_{12}, b_{10} are arbitrary real numbers.

We choose particular values to illustrate rogue waves solution to (2+1)-dimensional eCBSL equation:

$$\beta = 4, a_0 = 1, a_{13} = \frac{1}{2}, a_{23} = -4, a_{20} = 4, a_{31} = 40, a_{30} = 2, b_{11} = 2, b_{12} = 1, b_{10} = 0, m_1 = 2. \tag{50}$$

The dynamic characters and structures of the rogue wave solution are vividly shown in figure 5 which contained the three-dimensional plots [see figure 5(a,b,c)] that exhibit the localized structures and contour plots [see figure 5(d,e,f)] in the (x, y)-plane when t = -2, -1, 0. This wave is composed of two parts including a higher-order rational

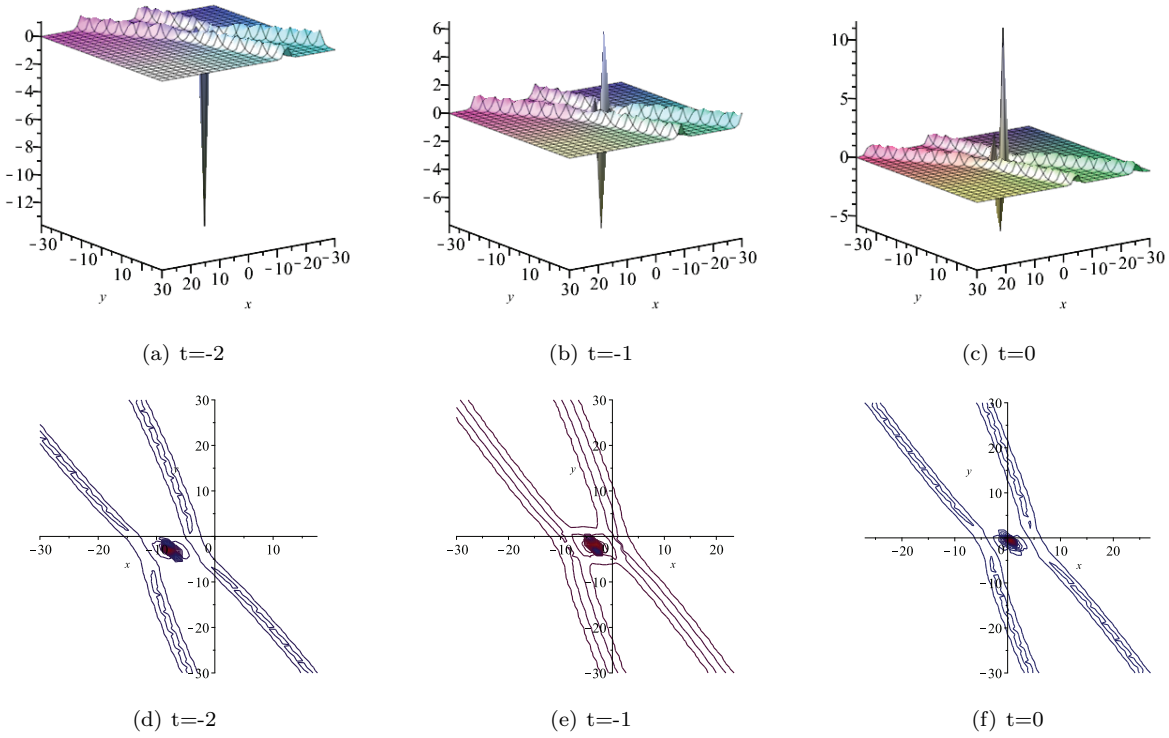

(a) t=-2 (b) t=-1 (c) t=0

(d) t=-2 (e) t=-1 (f) t=0

Figure 5: Three-dimensional plots and contour maps of the wave with the parameters (50) at times t = -2, -1, 0.

wave and other functions wave (double-exponential function, tangent function and tanh function). As we have seen, the higher-order rational wave, double exponential function, tangent function and tanh function waves react with each other finely and keep moving forward while the height of higher-order rational wave increases with time.

6 Conclusion

In this paper, we constructed an original form of exact analytical solutions to nonlinear evolution equation with the aid of bilinear neural network method and several examples were given to illustrate the methodology. We were of free choice to the number of N and M, the order of φ, the hidden layer of $g(\psi)$ and the weight coefficients in the expression (3), for instance, we derived the high-order lump-type solutions when $N = 3, n_1 = 2, n_3 = n_2 = 1, m_j = 0$ in (3), the higher-order rational solutions when $N = 3$, $n_1 = 4, n_3 = 2, n_2 = 1, m_j = 0$ in (3), the periodic wave solutions when $a_{ik} = 0$, $m_4 = m_3 = m_2 = m_1$, $\psi_2 = \psi_1$, $g_3(\psi_3) = \tan\psi_3, g_4(\psi_4) = \tanh\psi_4$ and when $a_{ik} = 0$, $m_2 = m_1$, $\psi_2 = \psi_1$, $g_3(\psi_3) = \cos\psi_3, g_4(\psi_4) = \sin\psi_4$ in (3), the breather solutions when $a_{ik} = 0$, $m_4 = 0$, $g_3(\psi_3) = \cos\psi_3$ in (3) and the rogue waves solutions of (2+1)-dimensional eCBSL equation. In particular, the results were identical when $N = 3$, $n_1 = 2p$, $n_2 = 2$, $n_3 = 1$, $m_i = 0$ $(p = 3, 4, 5, 6)$, and so did the results when $N = 3$, $n_1 = 2q$, $n_2 = 3$, $n_3 = 1$, $m_i = 0$ $(q = 4, 5, 6)$, etc. The exact analytical solutions were widely expanded due to choosing different basic functions of the hidden layer and the order of the terms. In addition to the results we obtained in this paper, our approach can be applied to calculate other types multiple solutions of NLEEs.

Acknowledgments

This work is supported by the National Natural Science Foundation of China (11661060, 12061054), Program for Young Talents of Science and Technology in Universities of Inner Mongolia Autonomous Region (NJYT-20-A06) and the Natural Science Foundation of Inner Mongolia Autonomous Region of China (2018LH01013).

References

[1] Wang ML, Zhou YB, Li ZB.Application of a homogeneous balance method to exact solutions of nonlinear equations in mathematical physics. *Physics Letters A*. 1996;216:67.

[2] Chen HH, Li YC, Liu CS. Integrability of nonlinear Hamiltonian systems by inverse scattering method. *Physica Scripta*. 1979;20(3-4):490.

[3] Hirota R, Satsuma J. A variety of nonlinear network equations generated from the Bäcklund transformation for the Toda lattice. *Supplement of the Progress of Theoretical Physics*. 1976.

[4] Li RM, Geng XG, Xue B. Darboux transformations for a matrix long-wave-short-wave equation and higher-order rational rogue-wave solutions. *Mathematical Methods in the Applied Sciences*. 2020;200:163348.

[5] Hirota R, Satsuma J. Soliton solution of a coupled KdV equation. *Physics Letters A*. 1981;85:407.

[6] Bilige SD, Chaolu TM, Wang XM. Application of the extended simplest equation method to the coupled Schrödinger-Boussinesq equation. *Applied Mathematics and Computation*. 2013;224:517.

[7] Tang X, Chen Y. Lumps, breathers, rogue waves and interaction solutions to a (3+1)-dimensional Kudryashov-Sinelshchikov equation. *Modern Physics Letters B*. 2020;34:2050117.

[8] Liu JG, Wazwaz AM. Breather wave and lump-type solutions of new (3+1)-dimensional Boiti-Leon-Manna-Pempinelli equation in incompressible fluid. *Mathematical Methods in the Applied Sciences*. 2020;10:1038-1046.

[9] Liu JG. Lump-type solutions and interaction solutions for the (2+1)-dimensional generalized fifth-order KdV equation. *Applied Mathematics Letters*. 2018;86:36-41.

[10] Issasfa A, Lin J. Lump and mixed rogue-soliton solutions to the 2+1 dimensional Ablowitz-Kaup-Newell-Segur equation. *Journal of Applied Analysis and Computation*. 2020;10:314-325.

[11] Liu YK, Li B, Wazwaz AM. Novel high-order breathers and rogue waves in the Boussinesq equation via determinants. *Mathematical Methods in the Applied Sciences*. 2016;6:367-375.

[12] Zhang RF, Bilige SD. New interaction phenomenon and the periodic lump wave for the Jimbo-Miwa equation. *Modern Physics Letters B*. 2019;33:1950067.

[13] Mi LF, Cui WY, You HL. Periodic and quasi-periodic solutions for the complex Swift-Hohenberg equation. *Journal of Applied Analysis and Computation*. 2020;10:297-313.

[14] Yue YF, Chen Y. Dynamics of localized waves in a (3+1)-dimensional nonlinear evolution equation. *Modern Physics Letters B*. 2019;33:1950101.

[15] Ma WX. Lump and Interaction Solutions of Linear PDEs in (3+1)-Dimensions. *East Asian Journal on Applied Mathematics*. 2019;9:185-194.

[16] Ma WX, Zhou Y. Lump Solutions to Nonlinear Partial Differential Equations via Hirota Bilinear Forms. *Journal of Differential Equations*. 2018;264(4):2633-2659.

[17] Chen ST, Ma WX. Lump solutions to a generalized Bogoyavlensky-Konopelchenko equation. *Frontier of Mathematic in China*. 2018;13(3):525.

[18] Lü X, Ma WX. Study of Lump Dynamics Based on a Dimensionally Reduced Hirota Bilinear Equation. *Nonlinear Dynamics*. 2016;85:1217-1222.

[19] Lü JG, Zhu WH. Multiple rogue wave solutions for (2+1)-dimensional Boussinesq equation. *Chinese Journal of Physics*. 2020;67:492-500.

[20] Zhao ZL, He LC. Multiple lump solutions of the (3+1)-dimensional potential Yu-Toda-Sasa-Fukuyama equation. *Applied Mathematics Letters*. 2019;95:114-121.

[21] Zhang RF, Bilige SD. Bilinear neural network method to obtain the exact analytical solutions of nonlinear partial differential equations and its application to p-gBKP equation. *Nonlinear Dynamic*. 2019;95:3041-3048.

[22] Wang XM, Bilige SD. Novel interaction phenomena of the (3+1)-dimensional Jimbo-Miwa equation. *Communications in Theoretical Physics*. 2020;72:04500.

[23] Zhou Y, Solomon M, Ma WX. Lump and lump-soliton solutions to the Hirota-Satsuma-Ito equation. *Communications in Nonlinear Science and Numerical Simulation*. 2019;68:56.

[24] Gai LT, Ma WX, Li MC. Lump-type solution and breather lump-kink interaction phenomena to a (3+1)-dimensional GBK equation based on trilinear form. *Nonlinear Dynamics*. 2020;100:2715-2727.

[25] Zhang RF, Bilige SD, Bai YX, Lü JQ, Gao XQ. Interaction phenomenon to dimensionally reduced p-gBKP equation.*Modern Physics Letters B*. 2018;32(06): 1850074.

[26] Yue YF, Huang LL, Chen Y. N-solitons, breathers, lumps and rogue wave solutions to a (3+1)-dimensional nonlinear evolution equation. *Computers and Mathematics with Applications*. 2018;75:2538.

[27] Ma WX. Generalized bilinear differential equation. *Studies in Nonlinear Sciences*. 2011;2:140.

[28] Ren B, Lin J, Lou ZM. A new nonlinear equation with lump-soliton, lump-periodic, and lump-periodic soliton solutions. *Complexity*. 2019; 2019:065206.